Supporting Information

Karunarathne et al. 10.1073/pnas.1220755110

SI Methods

Constructs. All DNA analysis was done using the National Center for Biotechnology Information and alignment of opsins was done using ClustalW software. Blue opsin (bOpsin) mCherry construct was created by subcloning bOpsin into the EcoRI-NotI and mCherry into the NotI-XbaI sites of pcDNA3.1 (Invitrogen). A synthetic chimera (CrBlue) was created (Integrated DNA Technologies) and subcloned into the EcoRI-NotI sites of pcDNA3.1. mCherry γ9 was made by subcloning mCherry into the HindIII-KpnI sites and γ9 into the KpnI-EcoRI sites of pcDNA3.1. Plasmids were transformed into Top10 cells (Invitrogen), using ampicillin as a selection marker, selected by PCR screening, and confirmed by sequencing YFP-γ9 as previously described. Blue opsin was provided by D. Oprian (Brandeis University, Waltham, MA), mGFP-Actin was from Ryohei Yasuda (Max Planck Florida Institute, Jupiter, FL; Addgene no. 21948), Akt-PH-GFP was from Craig Montell (The Johns Hopkins University School of Medicine, Baltimore; Addgene no.18836), EGFP-Rac1 was from Gary Bokoch (The Scripps Research Institute, La Jolla, CA; Addgene no.12980), EGFP-Rac1-T17N was from Gary Bokoch (Addgene no.12982), and GFPΔ-epac-mCherry (mCh) cAMP sensor was from K. Jalink (The Netherlands Cancer Institute, Amsterdam)

Data Analysis Software and Statistics. All intensity recordings were background subtracted. Image analysis was performed using Andor IQ v2.4.1 and task-specific Python scripts. Data analyses, curve fitting, and statistical analysis associated with the corresponding functions were performed using OriginPro 8.6/9.0 and Matlab (R2011b). Cell and optical input coordinates were determined using the Tracker video analysis and modeling tool. Detail statistical analyses are described in the *Methods* section in the main text. Error bars represent mean ± SEM or SD as stated.

Imaging Setup. For imaging, cells were seeded in 29-mm glass-bottom tissue culture dishes. Hanks' balanced salt solution (HBSS) supplemented with 1g/L glucose was used as the imaging buffer in all experiments. All imaging was performed with a spinning-disk confocal imaging system comprising a Leica DMI6000B inverted microscope; a Yokogawa CSU-X1 spinning-disk unit; an Andor fluorescence recovery after photobleaching and photoactivation (FRAPPA) unit; a laser combiner with 50-mW 445-, 488-, 515-, and 594-nm solid-state lasers; and an iXon+ EMCCD camera. This system is capable of high-speed 4D image acquisition, exposing a stationary or moving selected area to a light beam of desired intensity and wavelength for defined durations of time and live data acquisition. The environmental chamber on the microscope was at 37 °C and dishes were masked with a transparent CO_2 mask to maintain humidified 5% CO_2 over the cells. Adaptive corrective focus was used to prevent focus drift during time-lapse imaging experiments. All imaging experiments were conducted using a 63×, 1.4HCX apochromat objective. In experiments involving opsin activation, dishes were kept completely in the dark from the time of addition of 11-*cis* retinal. Depending on the opsin, wavelengths other than its λ-max were used to visualize cells.

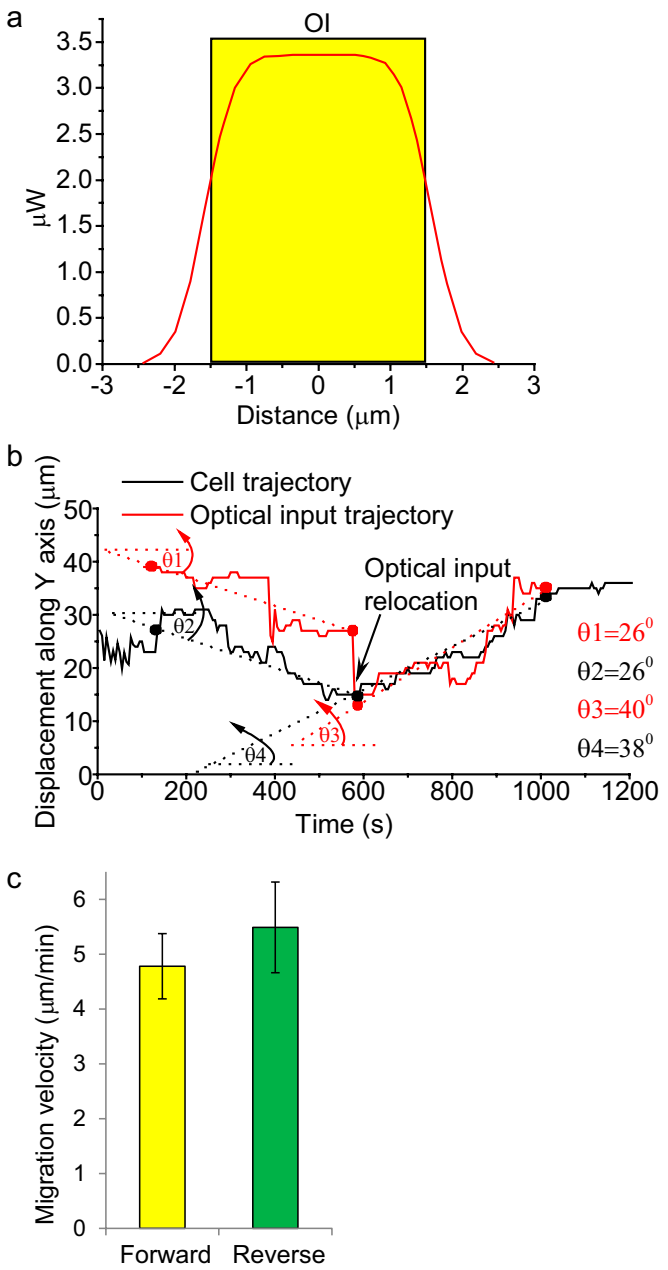

Fig. S1. (*A*) Cross-sectional energy distribution of a 3 × 3-μm^2 optical input created using a 445-nm laser with beam intensity of 5 μW at the image plane. (*B*) Representative directional coupling of cell and optical input trajectories along the *y* axis due to displacement of optical input and cell during forward movement (θ1, θ2) and reverse movement (θ3, θ4) ($n = 3$). (*C*) Optically induced average forward ($n = 6$) and reverse ($n = 5$) migration velocities of RAW 264.7 cells expressing bOpsin. Error bars: Mean ± SEM.

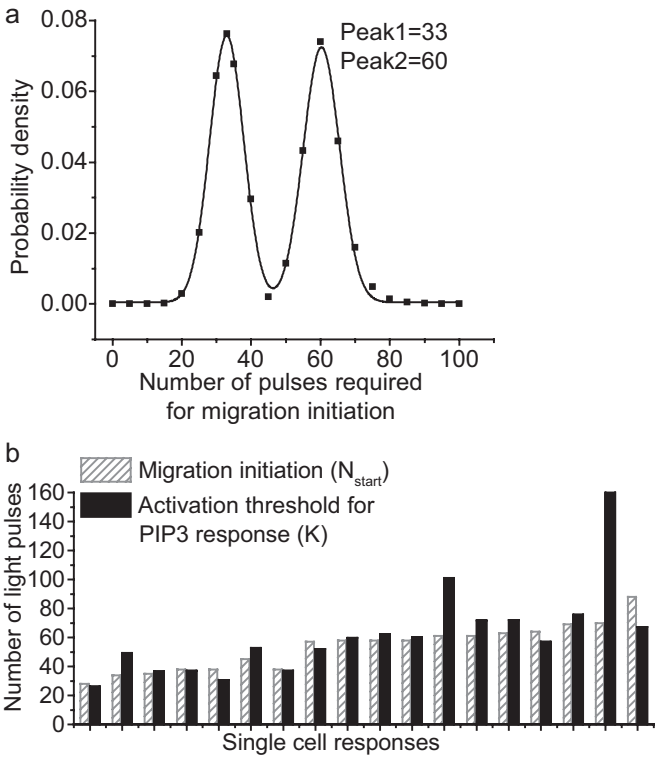

Fig. S2. (*A*) Population analysis of 23 cells based on input required for migration initiation indicates a bimodal distribution (cut point = 46) (Fig. 6*C*). (*B*) Bar chart showing activation threshold for the phosphatidylinositol (3,4,5)-triphosphate (PIP3) response (*K*) and input required for migration initiation for individual cells.

Table S1. Systems parameters for PIP3 response

	Group 1		Group 2		Pooled population	
Value	Mean	SEM	Mean	SEM	Mean	SEM
n_H	3.9	0.4	4.4	0.6	4.2	0.4
K	38.7	4.2	77.2	9.2	64.4	7.6
N_{peak}	63.2	5.0	86.6	5.4	79.2	4.7
N_{start}	36.3	2.35	64.5	2.5	55.1	3.7

Pooled population: Entire population that shows migration. Grouped population: Grouping of cells on the basis of N_{start} (the number of pulses required to initiate the cell migration). Values of mean and SEM for Hill coefficient (n_H), activation threshold (K), number of light pulses required to reach the peak PIP3 response (N_{peak}), and N_{start} are reported.

Table S2. Description of model variables

Variable	Description
G_F	Activated G protein in front
A_{mF}	Activator at the membrane in front
I_{cytF}	Inhibitor in cytosol in front
I_{mF}	Inhibitor at the membrane in front
$PIP3_F$	PIP3 concentration in front
G_B	Activated G protein in back
A_{mB}	Activator at the membrane in back
I_{cytB}	Inhibitor in cytosol in back
I_{mB}	Inhibitor at the membrane in back
$PIP3_B$	PIP3 concentration in back

Table S3. List of model parameters used in this study

Parameter	Description	Value	Unit
S_F	Stimulus at front	0.1	Dimensionless
S_B	Stimulus at back	0	Dimensionless
$k0$	G-protein activation	0.04	1/s
$k0r$	G-protein deactivation	0.02	1/s
$k1$	Activator formation	1.00	μM/s
$k2$	Inhibitor formation	0.01	μM/s
$k1r$	Activator and inhibitor deactivation	0.2	1/s
krm	Inhibitor recruitment rate from cytosol to membrane	0.25	1/s
$k2r$	Deactivation due to antagonism	0.2	1/(μM*s)
$k3$	PIP3 formation	0.20	1/s
$k3r$	PIP3 disappearance	0.20	1/(μM*s)
$k30$	Basal PIP3 formation	0.05	μM/s
$k30r$	Basal PIP3 degradation	0.05	1/s
kt	Inhibitor translocation	10	1/s
km	Half-saturation constant for G protein for activator and inhibitor	0.50	μM
G_T	Total G protein	0.5	μM
V_c	Correction factor for effective volumes corresponding to cytosol and membrane	100	Dimensionless

Table S4. Initial conditions of model components

Initial conditions	Description	Value/μM
G_F	G protein at front	0
A_{mF}	Activator at membrane at front	0
I_{cytF}	Inhibitor in cytosol at front	0
I_{mF}	Inhibitor at membrane at front	0
$PIP3_F$	PIP3 at front	1
G_B	Activated G protein in back	0
A_{mB}	Activator at the membrane in back	0
I_{cytB}	Inhibitor in cytosol in back	0
I_{mB}	Inhibitor at the membrane in back	0
$PIP3_B$	PIP3 concentration in back	1

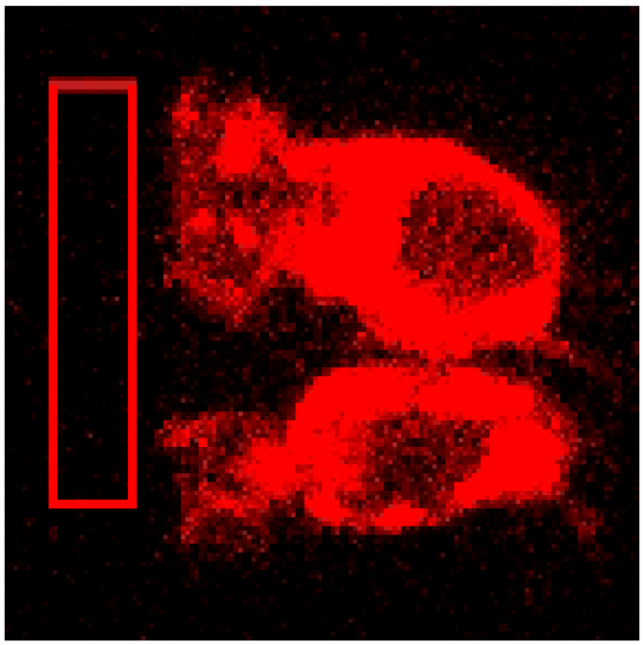

Movie S1. Optical activation directs cell migration. RAW 264.7 cells expressing bOpsin-mCh were imaged for mCh every 5 s. Immediately after optical activation at 445 nm (red box), cells formed protrusions in the direction of optical activation (OA) and continued to follow the optical path. At the end of the field, the two cells were then activated with two separate and restricted optical inputs (one per cell) at opposing ends. At this point cells continued to move in the new direction of optical input movement. Two movies are stitched. The first movie ends with suspension of OA of the top cell. The second movie starts 30 s later and is noted in time resetting to zero.

Movie S1

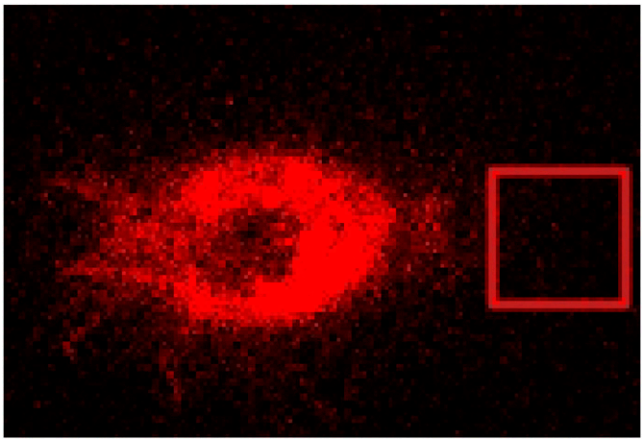

Movie S2. Optical activation induces complete cell migration reversal. RAW 264.7 cells expressing bOpsin-mCh were imaged for mCh every 5 s. The cell initially followed the direction of OA and migrated to the left. At 09:35 (min:s), movement directionality of the optical input was changed by 180° (from front to back of the cell), resulting in termination of the cell's leftward movement and initiation of lamellipodia toward new optical input. Subsequent frames show lamellipodia collapse at the initial front and complete cell migration toward the new optical input, transforming the initial front to back and vice versa.

Movie S2

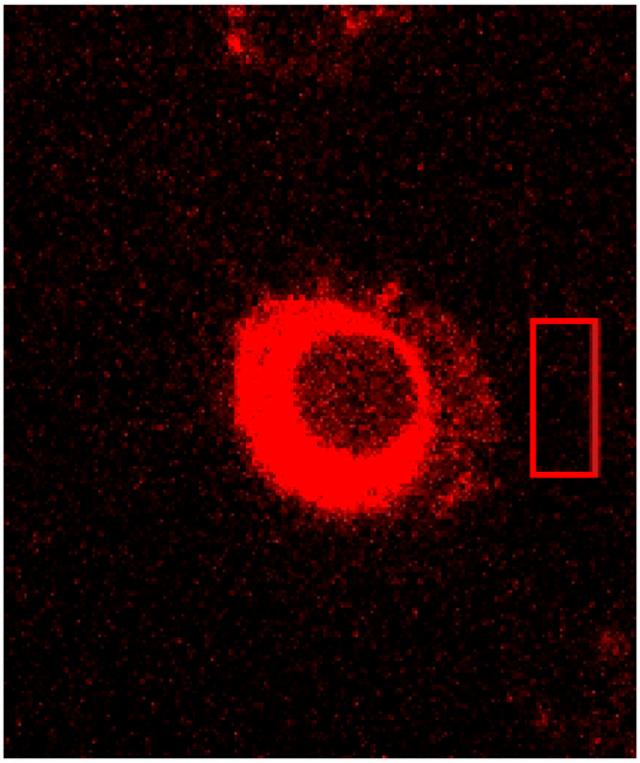

Movie S3. Sequential optical activation steers migration in four different directions. A RAW 264.7 cell expressing bOpsin-mCh was imaged for mCh every 5 s. Cells formed directionally sensitive lamellipodia immediately after optical activation at 445 nm (red box) and migrated toward the optical input (OI). After the first two directional activations, cells were imaged for a period without OA.

Movie S3

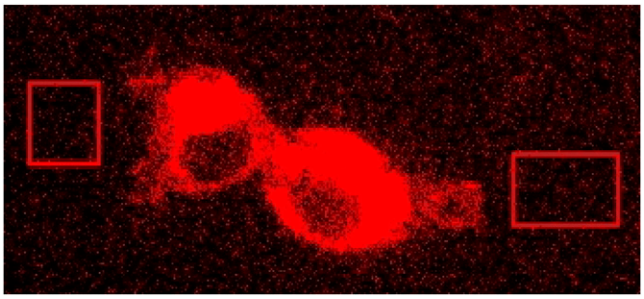

Movie S4. Attached cells were optically activated simultaneously (red boxes). Cells independently followed the opposing optical paths. RAW 264.7 cells expressing bOpsin-mCh are shown.

Movie S4

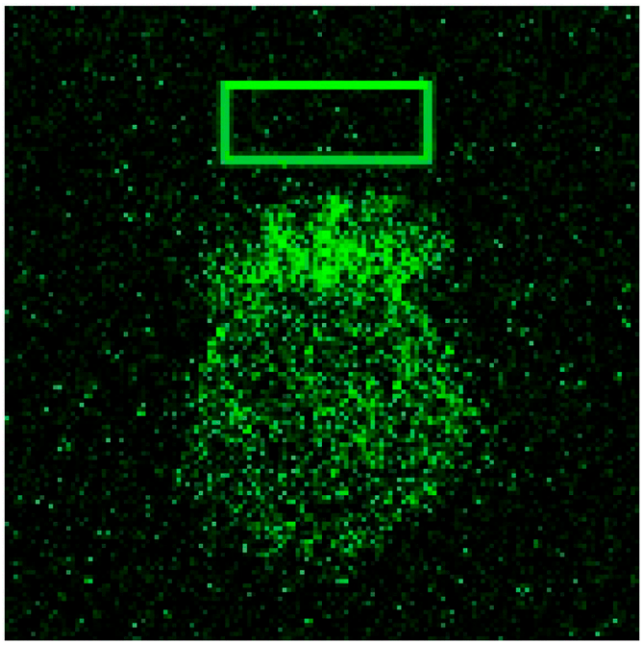

Movie S5. Continuous monitoring of PIP3 dynamics during optically induced immune cell migration. Shown is the initiation and maintenance of PIP3 gradient parallel to the migratory response. A RAW 264.7 cell transfected with bOpsin-mCh and PIP3 sensor, Akt-PH-GFP was imaged for GFP every 1 s. Stationary optical input (445 nm, green box) pulsed every 1 s.

Movie S5

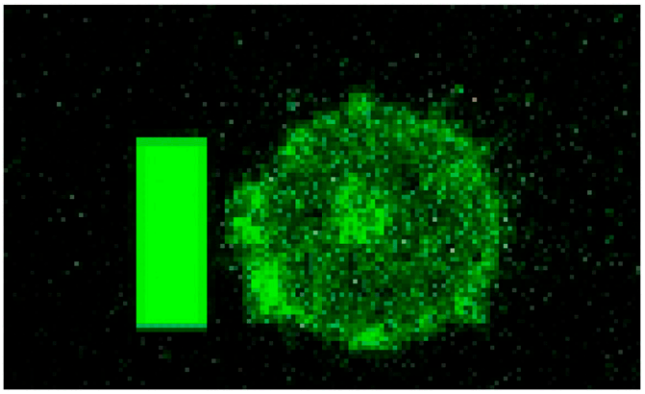

Movie S6. Formation of the leading edge by optical activation of RAW 264.7 cells expressing bOpsin-mCh (red) and β-actin-GFP (green). Green box is the optical input. Actin accumulates rapidly proximal to light (front) while it disappears from the back of the cell.

Movie S6

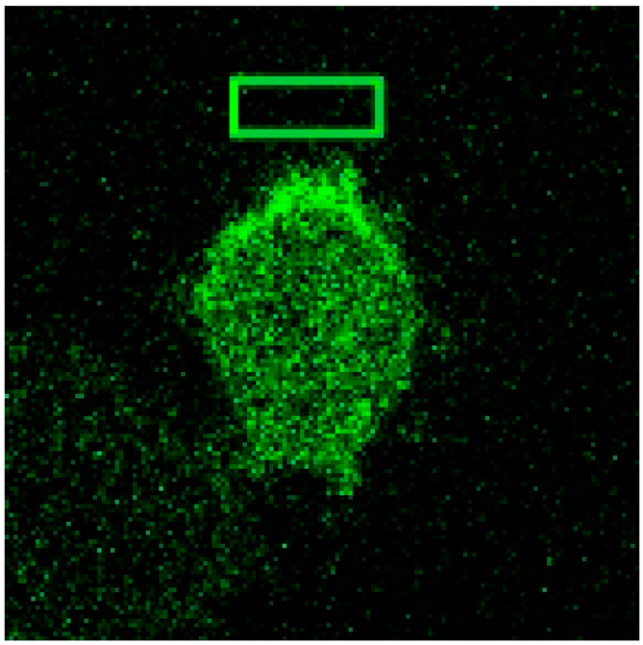

Movie S7. Optical input sets up PIP3 gradient (increase at the front and decrease at the back) across the cell. A RAW 264.7 cell transfected with bOpsin-mCh and PIP3 sensor, Akt-PH-GFP was imaged for GFP every 1 s. Optical input (445 nm, green box) pulsed every 1 s induced PIP3 increase at the front and a simultaneous decrease at the back accompanying cell migration initiation. Note that switching the optical input by 180° resulted in reversal of the PIP3 gradient between front and back. Repeated switching demonstrates that cell polarization is not permanent and can be reversed.

Movie S7